IOP Publishing | Bureau International des Poids et Mesures
Metrologia
Metrologia 52 (2015) S305–S313
doi:10.1088/0026-1394/52/5/S305

Measurement of pressures up to 7 MPa applying pressure balances for dielectric-constant gas thermometry

Thorsten Zandt, Wladimir Sabuga, Christof Gaiser and Bernd Fellmuth

Physikalisch-Technische Bundesanstalt (PTB), Abbestrasse 2–12, 10587 Berlin, and Bundesallee 100, 38116 Braunschweig, Germany

E-mail: Christof.Gaiser@PTB.de

Received 9 February 2015, revised 8 June 2015
Accepted for publication 9 June 2015
Published 19 August 2015

Abstract

For the determination of the Boltzmann constant by dielectric-constant gas thermometry, the uncertainty of pressure measurements in helium up to 7 MPa has been decreased compared with previous achievements (Sabuga 2011 *PTB-Mitt.* **121** 247–55). This was possible by performing comprehensive cross-float experiments with a system of six special pressure balances and the synchronization of their effective areas. It is now possible to measure a helium pressure of 7 MPa with a relative standard uncertainty of 1.0 ppm applying a 2 cm^2 piston-cylinder unit, the calibration of which is traceable to the SI base units.

Keywords: gas pressure balance, effective area, pressure distortion coefficient, dielectric-constant gas thermometry, Boltzmann constant

(Some figures may appear in colour only in the online journal)

1. Introduction

The determination of the Boltzmann constant k by dielectric-constant gas thermometry (DCGT) is directed to the new definition of the base unit kelvin, which is planned to come into force in 2018 [2]. For this goal, a relative uncertainty below 3 ppm is necessary [3]. In turn, this requires to measure pressures up to 7 MPa with a relative uncertainty of order one part per million (1 ppm) [4]. To achieve this level, a project was started at PTB to improve the national pressure standard accordingly. The solution for this improvement and the first results obtained in 2011 are summarized in section 2. The first results were the starting point for activities performed in 2013 and 2014 to finally decrease the uncertainty to 1 ppm. These activities are described in detail in the following sections 3 and 4. After establishing a complete uncertainty budget in section 5, conclusions are drawn and an outlook is given at the end of the paper.

2. Improvement of the national pressure standard of the PTB in 2011

The goal to measure pressures up to 7 MPa with a relative uncertainty of order 1 ppm is achievable only by using pressure balances, which act moreover as pressure stabilisers. A system of special pressure balances, as outlined in [1, 5], was designed, constructed, and evaluated [6–8], see also the summary in [9]. The system includes two pressure-balance platforms, three piston-cylinder units (PCUs) with effective areas of 20 cm^2 (Nos. 1159, 1162, and 1163), and three 2 cm^2 PCUs (Nos. 1341, 1342, and 1343). Traceability to the SI base units up to 7 MPa was realized in two general steps. First, the zero pressure effective areas of the 20 cm^2 PCUs were determined from dimensional measurements. Second, the 2 cm^2 PCUs were calibrated against the 20 cm^2 PCUs by cross-float comparisons. The calibration of the mass pieces traceable to the national mass standards and the accurate

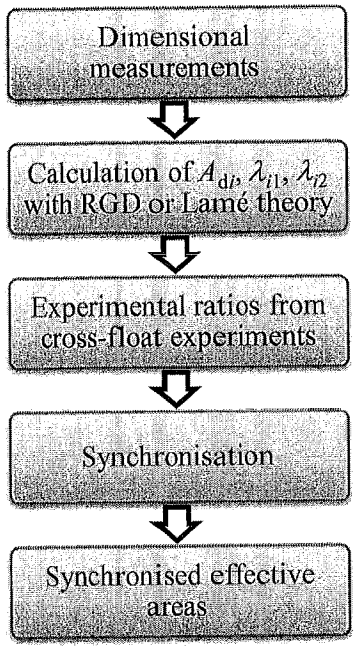

Figure 1. Detailed steps of the traceable calibration of the 2 cm^2 PCUs. A_{di} is the dimensional effective area of PCU No. i at zero pressure. λ_{i1} and λ_{i2} are the coefficients describing the non-linear distortion of the PCUs under pressure. They are calculated by applying the RGD theory [8] or the Lamé theory [10].

determination of the local gravity acceleration did not cause any special challenges.

The detailed steps of the traceable calibration of the 2 cm^2 PCUs are illustrated in figure 1. The dimensional data for the 2 cm^2 PCUs are first of all needed for the calculation of their pressure distortion coefficients by the finite element method [7]. The calculations are performed applying the rarefied gas dynamics (RGD) theory [8] or the Lamé theory [10]. Cross-float experiments are described in section 3, and the synchronization of effective areas in section 4.

Cross-float measurements determine the ratio of the effective areas of two PCUs at given pressures. They cannot yield the absolute areas, or the pressure dependence of the areas. Besides the area ratios, the measurements provide an information on the performance of the PCUs, especially an estimate of the Type A uncertainty contributions to pressure-balance readings. For performing the measurements, the PCUs are mounted on a common pressure system and are in equilibrium at the chosen pressure, when the pistons are loaded with appropriate masses and located at a defined reference level. Pressure balances act as barostats, i.e. they fix the pressure at the value defined by the applied load and the effective area. The basis of the comparison is, therefore, the determination of the loads, at which each balance would individually barostat the system at precisely the same pressure. In reality, the pressure-sensing technique was applied. The two pressure balances were individually barostatted by the PCUs, and the difference between the two pressures was measured with a differential-pressure indicator.

The results obtained in 2011 are described in detail in [1] and compared with the present results in the following two sections, see tables 1 and 4. They yielded a combined standard uncertainty of the measurement of a helium pressure of 7 MPa using one of the 2 cm^2 PCUs (No. 1342) of 1.9 ppm, see the uncertainty budget given in [9] (table 1). The budget is dominated by the two components connected with zero-pressure effective area (1.5 ppm) and the pressure-distortion coefficient (1.1 ppm). The second dominating component was caused by an unexpected difference in the pressure dependence of the effective areas of two 2 cm^2 PCUs (Nos. 1342 and 1343). The present data show that this difference was obviously an experimental artefact, see figure 8 in the next section.

3. Cross-float measurements in 2013 and 2014

The second cross-float measurements campaign, being the topic of this paper, lasted about one year, namely from July 2013 to August 2014. It was performed to decrease the uncertainty of the pressure measurement up to 7 MPa by including all 6 PCUs, by clarifying the discrepancy between the pressure distortions of PCUs Nos. 1342 and 1343 obtained in the first campaign, see section 2, and by checking the long-term stability of the PCUs. Since the cross-float effective-area ratios R_{ij} fulfil the relations $R_{ij} = 1/R_{ji}$, a complete list of all possible cross floats includes 15 comparisons for the 6 PCUs (see figure 2): 3 comparisons of three pairs of 20 cm^2 PCUs in the pressure range from 0.15 MPa to 0.76 MPa, 9 comparisons between three 20 cm^2 PCUs and three 2 cm^2 PCUs (0.3 MPa to 0.76 MPa), and 3 comparisons of three pairs of 2 cm^2 PCUs (0.3 MPa to 7 MPa). All comparisons were performed in absolute mode with helium as measuring gas and applying a calibrated capacitive diaphragm gauge (CDG) for measuring the remaining pressure differences. The steps of the automated cross-float process are described in detail in [6].

Two CDGs with different operation ranges were used: First, a high-accuracy MKS Baratron capacitance diaphragm sensor (Model 698A11TRA, $u(\Delta p) = 0.1$ Pa) with a maximum line pressure of around 1 MPa and a useable differential pressure range of Δp of ± 1.3 kPa was used for all 15 comparisons. For the comparisons of three pairs of 2 cm^2 PCUs, of course comparisons only up to a maximum pressure of 1 MPa were carried out with this CDG. Secondly, a differential pressure transmitter from Rosemount (Series 3051 S, $u(\Delta p) = 0.25$ Pa) with a maximum line pressure of around 13.8 MPa and a useable differential pressure range of ± 5.0 kPa was applied for the comparisons up to a maximum pressure of 7 MPa. In the overlap range of the two CDGs (0.3 MPa to 1 MPa), no significant differences in the differential-pressure data were observed.

The calibration of the MKS Baratron capacitance diaphragm sensor was done traceable to the PTB primary standard for low pressures applying a Furness Rosenberg FRS4, which is a non-rotating force-balanced pressure balance [11]. The Rosemount differential pressure transmitter was calibrated by the twin pressure balance method [12] using two of the 20 cm^2 PCUs. For each differential pressure Δp, it was switched several times between Δp and zero pressure difference. This allows the removal of the influence of drifts and is called in [13] the 'ABABA' method.

Table 1. Cross-float effective-area ratios (R_{ij}) at zero pressure together with the associated relative uncertainties u_{Rij}, number of single samples (n_s), number of pressure values (n_p), and number of measurement series (n_m). For comparison purposes, the results obtained in the first cross-float measurements campaign published in 2011 [1] are also listed together with the deviation from the actual results.

	2014					2011		
PCU_i/PCU_j	R_{ij}	u_{Rij} in ppm	n_s	n_p	n_m	R_{ij}	u_{Rij} in ppm	ΔR_{ij} in ppm
1159/1162	1.00000368	0.42	159	8	4	1.00000342	0.64	− 0.26
1159/1163	0.99998476	0.45	171	8	5	0.99998441	0.67	− 0.35
1159/1341	9.99978201	0.74	294	7	8			
1159/1342	9.99928323	0.79	231	7	8	9.99929664	0.83	1.34
1159/1343	9.99956376	0.79	294	7	9	9.99957774	0.87	1.40
1162/1163	0.99998087	0.45	177	9	5	0.99998100	0.50	0.13
1162/1341	9.99974738	0.70	315	7	8			
1162/1342	9.99925406	0.76	294	7	7	9.99925931	0.84	0.53
1162/1343	9.99953286	0.80	294	7	7	9.99953954	0.87	0.67
1163/1341	9.99993519	0.69	252	7	6			
1163/1342	9.99944028	0.70	168	7	4	9.99944614	0.83	0.59
1163/1343	9.99972056	0.77	210	7	5	9.99973051	0.82	1.00
1341/1342	0.99995049	1.07	456	19	8			
1341/1343	0.99997971	1.85	609	19	11			
1342/1343	1.00002785	0.74	618	19	10	1.00002709	0.96	− 0.76

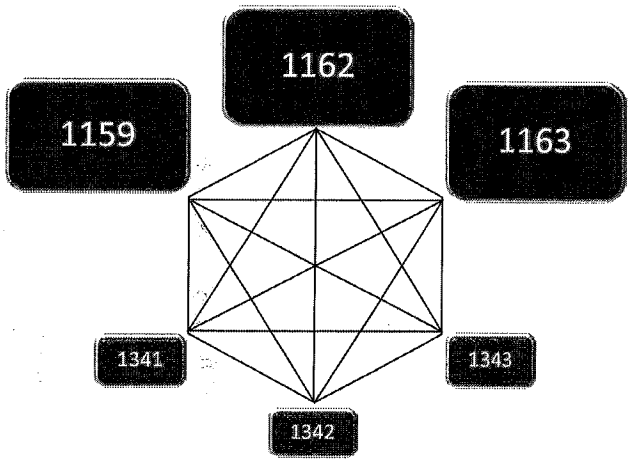

Figure 2. Complete scheme of the cross-float comparisons between the 6 PCUs.

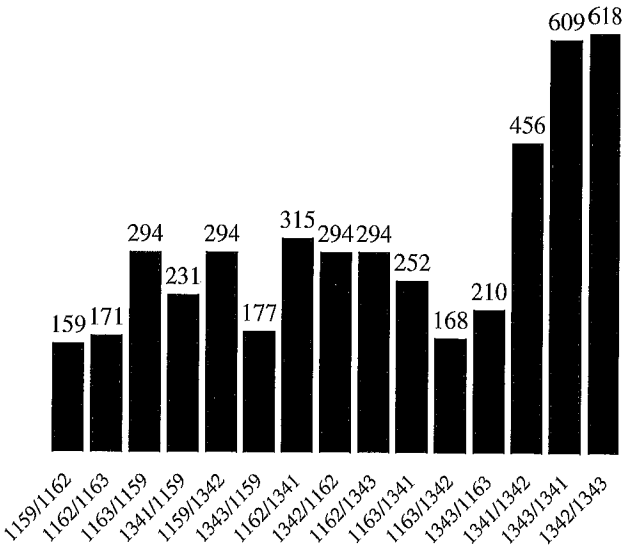

Figure 3. Histogram of the single samples of cross-float measurements of the 15 PCU pairs.

Overall, 4542 cross-float ratios R_{ij} (single samples) were measured, see table 1 and figure 3, where for each comparison pair at least 159 single samples were taken at 7 pressures or more during at least 4 measurement series (individual automated cross-float processes). Thus, the data give sufficient information on the repeatability and sensitivity of both the PCUs and the CDGs. For comparison purposes, in table 1 the results obtained in the first cross-float measurements campaign are also listed. Their deviation from the actual results is well within the expanded (coverage factor two) combined uncertainty. An additional check is the requirement that the complete product of the corresponding cross-float ratios should be equal to one. This is sufficiently fulfilled for the 20 cm^2 PCUs at a level of 0.2 ppm, and for the 2 cm^2 PCUs of 1 ppm. These deviation levels are in accordance with the complete uncertainty budget for the cross-float results, which is given in table 2. The pressure dependence of the measured effective areas A_i is shown in figures 4 to 9 for the six PCUs. In each case, the drawn A_i values were deduced from the single-sample cross-float ratios R_{ij} using the synchronized A_j value of the respective counterpart that is given in section 4. Since the A_j values are primarily determined by the results of the cross-float measurements with the 20 cm^2 PCUs up to 0.76 MPa, the effective-area values A_i obtained for the 2 cm^2 PCUs at higher pressures up to 7 MPa are partly not symmetric to the synchronized areas, and many data are out of the standard confidence interval. The distortion of the PCUs under pressure is considered using the pressure dependent coefficients $\lambda_i(p) = (A_i(p) - A_i(p = 0\,\text{Pa}))/(A_i(p = 0\,\text{Pa})p) = \lambda_{i1} + \lambda_{i2}p$ listed in table 3.

4. Synchronization of effective areas

Compared with the dimensional data, the effective-area ratios determined by the cross-float measurements provide additional

Table 2. Type B uncertainty budget for the effective areas ratio $R_{1342,\,1162}$ of PCUs Nos. 1342 and 1162. The relative uncertainty components are given in parts per million (ppm). The temperature of the PCUs was measured applying platinum resistance thermometers (PRTs). The temperature inhomogeneity was estimated comparing the readings of two PRTs for each PCU.

Quantity	Uncertainty	$u_B(R_{ij})$ in ppm
Room temperature	$4.0 \cdot 10^{-1}$ °C	0.010
Gas density fluid for height difference	$1.0 \cdot 10^{-3}$	0.022
Residual pressure in 1162	$2.0 \cdot 10^{-3}$ Pa	0.004
Residual pressure in 1342	$2.0 \cdot 10^{-3}$ Pa	0.004
Height difference	$2.8 \cdot 10^{-1}$ mm	0.005
PRT calibration in 1162	$6.0 \cdot 10^{-3}$ °C	0.054
PRT calibration in 1342	$6.0 \cdot 10^{-3}$ °C	0.054
Temperature inhomogeneity in 1162	$2.9 \cdot 10^{-2}$ °C	0.150
Temperature inhomogeneity in 1342	$3.6 \cdot 10^{-2}$ °C	0.190
Calibration uncertainty of CDG	$1.0 \cdot 10^{-1}$ Pa	0.208
Standard deviation of CDG	$0.5 \cdot 10^{-1}$ Pa	0.017
Thermal expansion coefficient of 1162	$2.2 \cdot 10^{-7}$ K^{-1}	0.070
Thermal expansion coefficient of 1342	$2.2 \cdot 10^{-7}$ K^{-1}	0.060
Distortion coefficient of 1162	$8.0 \cdot 10^{-8}$ MPa^{-1}	0.042
Distortion coefficient of 1342	$4.2 \cdot 10^{-8}$ MPa^{-1}	0.022
Verticality of 1162	$4.0 \cdot 10^{-1}$ mm m^{-1}	0.080
Verticality of 1342	$4.0 \cdot 10^{-1}$ mm m^{-1}	0.080
Cylinder + weight carrier mass of 1162	$0.9 \cdot 10^{-6}$ kg	0.009
Cylinder + weight carrier mass of 1342	$0.4 \cdot 10^{-6}$ kg	0.042
Main ring weights of 1162	$1.3 \cdot 10^{-5}$ kg	0.086
Main ring weights of 1342	$2.4 \cdot 10^{-6}$ kg	0.510
Combined standard uncertainty		0.63

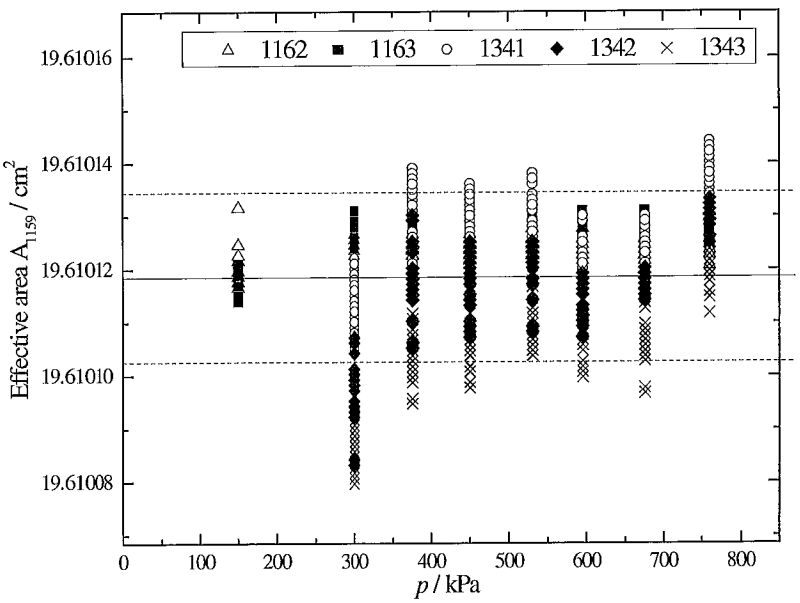

Figure 4. Effective area of the 20 cm^2 PCU No. 1159 versus pressure deduced from the cross-float measurements with the other five PCUs. The solid line shows the synchronized value given in table 4, and the dashed lines give the standard confidence interval (coverage factor $k = 1$).

(redundant) data on the values of the effective areas of the PCUs. Then it is of course desirable to determine the synchronized effective areas, which are as consistent as possible both with the initial dimensional effective areas and with the cross-float ratios. A suitable synchronization method is described in [14]. The approach is based on the weighted least squares method. As the criterion for the best synchronization, the minimization of the sum S of squared weighted differences between the input and output data, i.e. between the initial A_{di} and the synchronized A_i effective area of PCU No. i ($i = 1, 2, \ldots n$) as well as between the ratios A_i/A_j and the cross-float ratios R_{ij} ($R_{ij} = 1/R_{ji}$, $R_{ii} = 1$), is used:

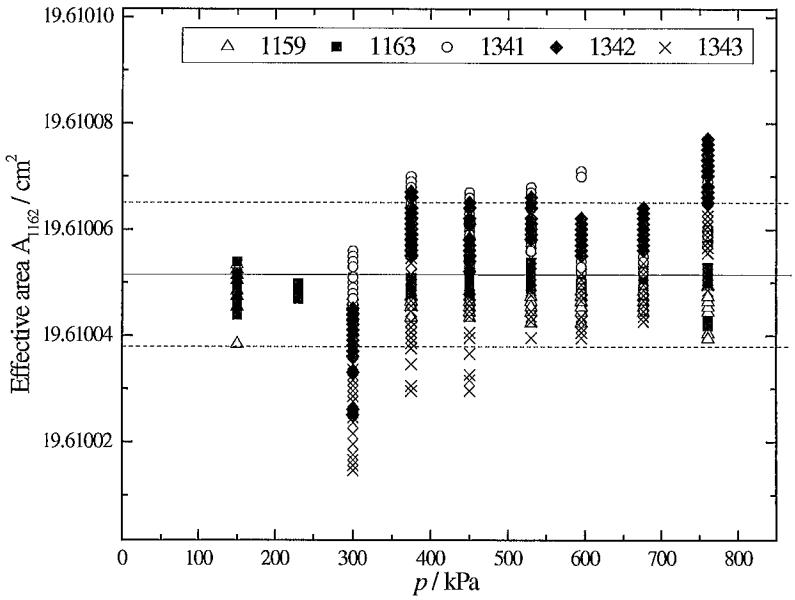

Figure 5. Effective area of the 20 cm^2 PCU No. 1162 versus pressure deduced from the cross-float measurements with the other five PCUs. The solid line shows the synchronized value given in table 4, and the dashed lines give the standard confidence interval ($k = 1$).

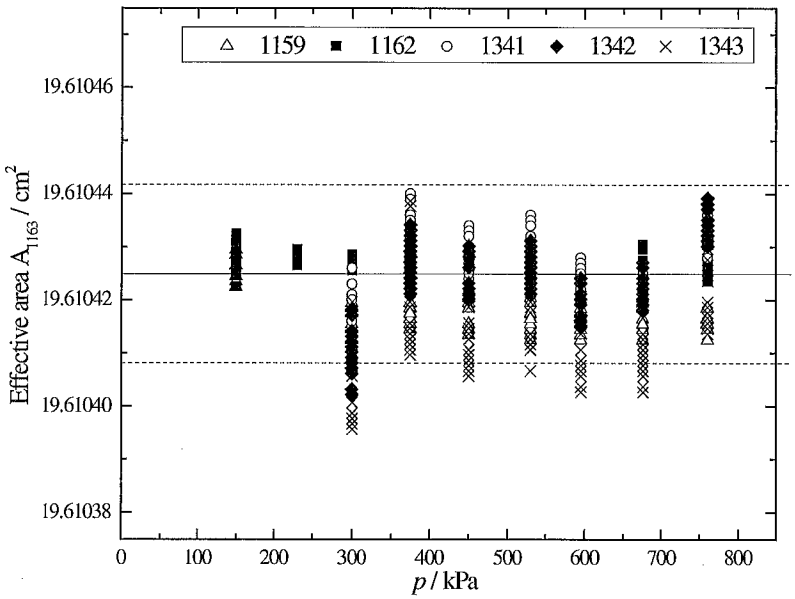

Figure 6. Effective area of the 20 cm^2 PCU No. 1163 versus pressure deduced from the cross-float measurements with the other five PCUs. The solid line shows the synchronized value given in table 4, and the dashed lines give the standard confidence interval ($k = 1$).

$$S = \sum_{i=1}^{n} \left(\frac{A_{\mathrm{d}i} - A_i}{A_{\mathrm{d}i} u_{\mathrm{d}i}} \right)^2 + \frac{1}{2} \sum_{\substack{i,j=1 \\ j \neq i}}^{n} \left(\frac{R_{ij} - A_i/A_j}{R_{ij} u_{Rij}} \right)^2 . \quad (1)$$

The input data are the $A_{\mathrm{d}i}$ and R_{ij} together with their relative uncertainties $u_{\mathrm{d}i}$ and u_{Rij} ($u_{Rij} = u_{Rji}$), whereas the output data are the A_i. The factor ½ before the second sum takes into account that due to $R_{ij} = 1/R_{ji}$, the ratio R_{ij} appears two times in equation (1). Sum S is minimal if the derivative $\partial S/\partial A_i = 0$ for all A_i. Apart from the factor two in the first term of numerator and denominator, the differentiation of equation (1) leads to the weighted mean

$$A_i = \frac{\dfrac{2A_{\mathrm{d}i}}{u_{\mathrm{d}i}^2} + \displaystyle\sum_{\substack{j=1 \\ j \neq i}}^{n} \frac{R_{ij} A_j}{(A_j/A_{\mathrm{d}i})^2 R_{ij}^2 u_{Rij}^2}}{\dfrac{2}{u_{\mathrm{d}i}^2} + \displaystyle\sum_{\substack{j=1 \\ j \neq i}}^{n} \frac{1}{(A_j/A_{\mathrm{d}i})^2 R_{ij}^2 u_{Rij}^2}} . \quad (2)$$

The factor two considers the fact that the input data for the cross-float measurements may be correlated to some extent, i.e. it increases the weight of the first term representing the direct dimensional data.

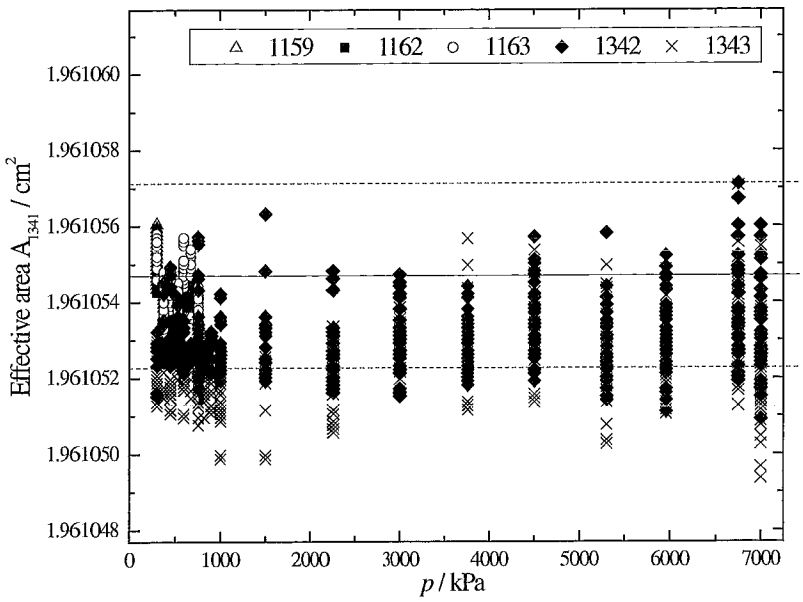

Figure 7. Effective area of the 2 cm^2 PCU No. 1341 versus pressure deduced from the cross-float measurements with the other five PCUs. The solid line shows the synchronized value given in table 4, and the dashed lines give the standard confidence interval ($k = 1$).

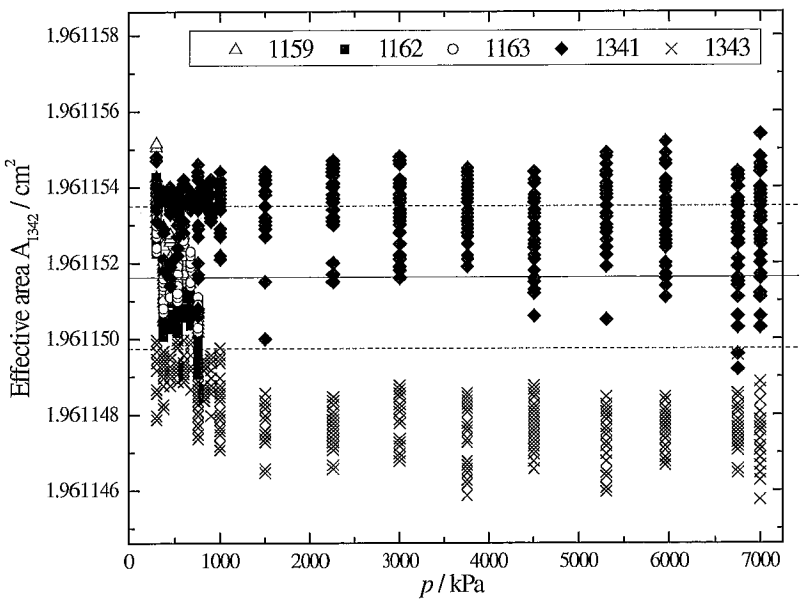

Figure 8. Effective area of the 2 cm^2 PCU No. 1342 versus pressure deduced from the cross-float measurements with the other five PCUs. The solid line shows the synchronized value given in table 4, and the dashed lines give the standard confidence interval ($k = 1$).

Taking into account that the term $(A_j/A_{di})\,R_{ij}$ is near to one ($(A_j/A_{di})\,R_{ij} \approx 1$), one gets

$$\left(\frac{2}{u_{di}^2} + \sum_{\substack{j=1 \\ j\neq i}}^{n} \frac{1}{u_{Rij}^2}\right) A_i - \sum_{\substack{j=1 \\ j\neq i}}^{n} \frac{R_{ij}}{u_{Rij}^2} A_j = \frac{2A_{di}}{u_{di}^2}, \qquad (3)$$

which is a system of linear equations $\boldsymbol{M} \times \boldsymbol{A} = \boldsymbol{A}_\mathbf{d}$ with the vectors $\boldsymbol{A} = (A_1, A_2, \ldots, A_n)^T$ and $\boldsymbol{A}_\mathbf{d} = \left(\frac{2A_{d1}}{u_{d1}^2}, \frac{2A_{d2}}{u_{d2}^2}, \ldots, \frac{2A_{dn}}{u_{dn}^2}\right)^T$. The elements of the $n \times n$ matrix $\boldsymbol{M}$ contain only the uncertainty estimates u_{di} and u_{Rij} as well as the ratios R_{ij}. This system can be solved by applying Cramer's rule:

$$A_i = \frac{\det(\boldsymbol{M}_i)}{\det(\boldsymbol{M})}, \qquad (4)$$

where the $n \times n$ matrix $\boldsymbol{M}_i$ results from $\boldsymbol{M}$ by replacing column i with vector $\boldsymbol{A}_\mathbf{d}$.

For the Type A relative standard uncertainty of the effective area A_i, $u_{Ai} = u_A(A_i)/A_i$, the following formula is given by Sabuga and Priruenrom [14]:

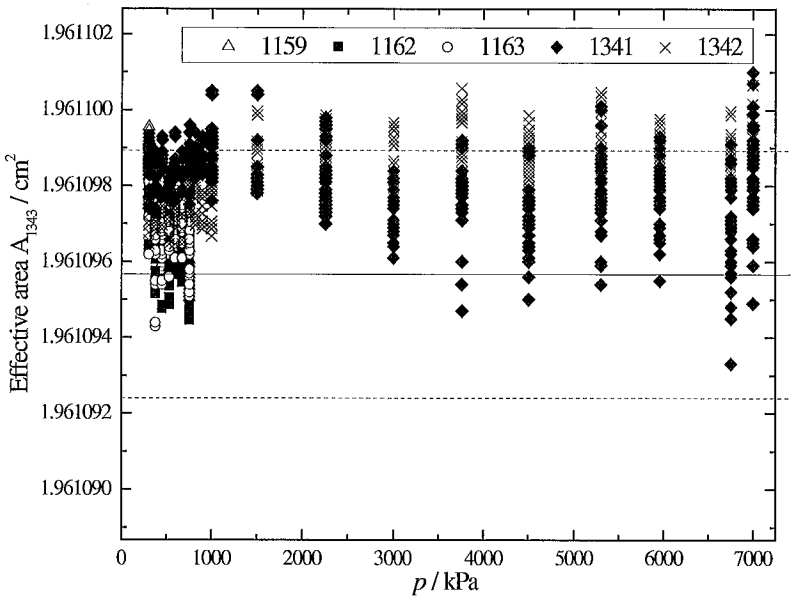

Figure 9. Effective area of the 2 cm^2 PCU No. 1343 versus pressure deduced from the cross-float measurements with the other five PCUs. The solid line shows the synchronized value given in table 4, and the dashed lines give the standard confidence interval ($k = 1$).

Table 3. Initial dimensional effective areas A_{di} at zero pressure with the associated relative standard uncertainties (u_{di}) and pressure distortion coefficients (λ_{i1} and λ_{i2}) based on dimensional measurements and, except for PCU 1341, calculated applying the finite element method and the RGD theory [7, 8]. The A_{di} value of PCU 1342 resulted from rather rough measurements. To get a reliable upper estimate, the given uncertainty covers the possible deviation from the nominal value. The pressure distortion coefficient $\lambda_{1341,1}$ for PCU 1341 was calculated with the Lamé theory [10]. For the pressure distortion coefficients, the uncertainties estimated at the maximum pressure are listed. With the exception of PCU 1341, the estimates $u(\lambda_i)$ consider only the uncertainty components due to the dimensional input data and the calculations. For PCUs 1342 and 1343, the pressure dependence of the cross-float ratio gives additional information, see text. For PCU 1341, the order of magnitude of $u(\lambda_i)$ has been estimated from the difference between the results obtained applying the Lamé and RGD theory, respectively, for PCUs 1342 and 1343.

PCU	A_{di} in cm^2	u_{di} in ppm	λ_{i1} in 10^{-6}MPa^{-1}	λ_{i2} in 10^{-6}MPa^{-2}	$u(\lambda_i)$ in 10^{-6}MPa^{-1}
1159	19.610112	0.7	6.854	− 2.064	0.10
1162	19.610058	0.5	6.406	− 1.930	0.08
1163	19.610439	0.6	5.969	− 2.147	0.10
1341	1.9610494	3.2	0.890		0.3
1342	1.961	500	0.999	0.028	0.034
1343	1.9610910	1.0	2.159	− 0.042	0.029

$$u_{Ai}^2 = \frac{n}{n-1} \frac{\left(\frac{A_{di}-A_i}{A_{di}u_{di}}\right)^2 + \frac{1}{2}\sum_{\substack{j=1 \\ j\neq i}}^{n}\left(\frac{R_{ij}-A_i/A_j}{R_{ij}u_{Rij}}\right)^2}{\frac{1}{u_{di}^2} + \frac{1}{2}\sum_{\substack{j=1 \\ j\neq i}}^{n}\frac{1}{u_{Rij}^2}}. \quad (5)$$

This is similar to the often used weighted standard deviation of the mean, see for instance [15]. But since again the data may be correlated to some extent, the factor n is added to the numerator. This factor guarantees a maximum estimation because u_{Ai} corresponding to equation (5) represents in fact the uncertainty of a single result. The formulas for the Type B relative standard uncertainty $u_{Bi} = u_B(A_i)/A_i$ of the effective area A_i result directly from equation (4) applying the law of propagation of uncertainty. They are presented in [14] (equations (9) to (14)). For obtaining a maximum estimate, the formula for correlated data has to be used. The combined relative standard uncertainty of A_i is of course given by $u_i = u(A_i)/A_i = (u_{Ai}^2 + u_{Bi}^2)^{0.5}$.

Using the dimensional effective areas given in table 3 and the cross-float ratios given in table 1 together with the respective uncertainty estimates as input data for equations (4), the synchronized effective areas listed in table 4 have been obtained. The Type A and B uncertainty components were estimated applying equation (5) and the formulas published in [14], respectively. Again, the new results are compared with those of the first campaign. Figure 10 illustrates the progress achieved by the synchronization.

To check the stability of the synchronization results, the following numerical tests and changes in the input data have been performed:

(i) Comparison of the results obtained applying the functions of Microsoft Excel for solving equations (4) with those obtained with a self-programmed MATLAB routine.

Table 4. Synchronized effective areas (A_i) resulting from the second cross-float measurements campaign, their Type A (u_{Ai}), Type B (u_{Bi}) and combined (u_i) relative standard uncertainties in ppm. For comparison purposes, the results obtained in the first cross-float measurements campaign are also listed.

	2014				2011			
PCU	A_i in cm^2	u_{Ai}	u_{Bi}	u_i	A_i in cm^2	u_{Ai}	u_{Bi}	u_i
1159	19.610118	0.44	0.69	0.81	19.610121	0.2	1.2	1.2
1162	19.610052	0.30	0.63	0.69	19.610056	0.2	1.1	1.1
1163	19.610425	0.54	0.66	0.86	19.610429	0.4	1.1	1.2
1341	1.9610547	0.53	0.80	0.96				
1342	1.9611516	0.45	0.76	0.88	1.9611503	0.6	1.3	1.5
1343	1.9610957	1.42	0.78	1.62	1.9610952	0.9	1.3	1.6

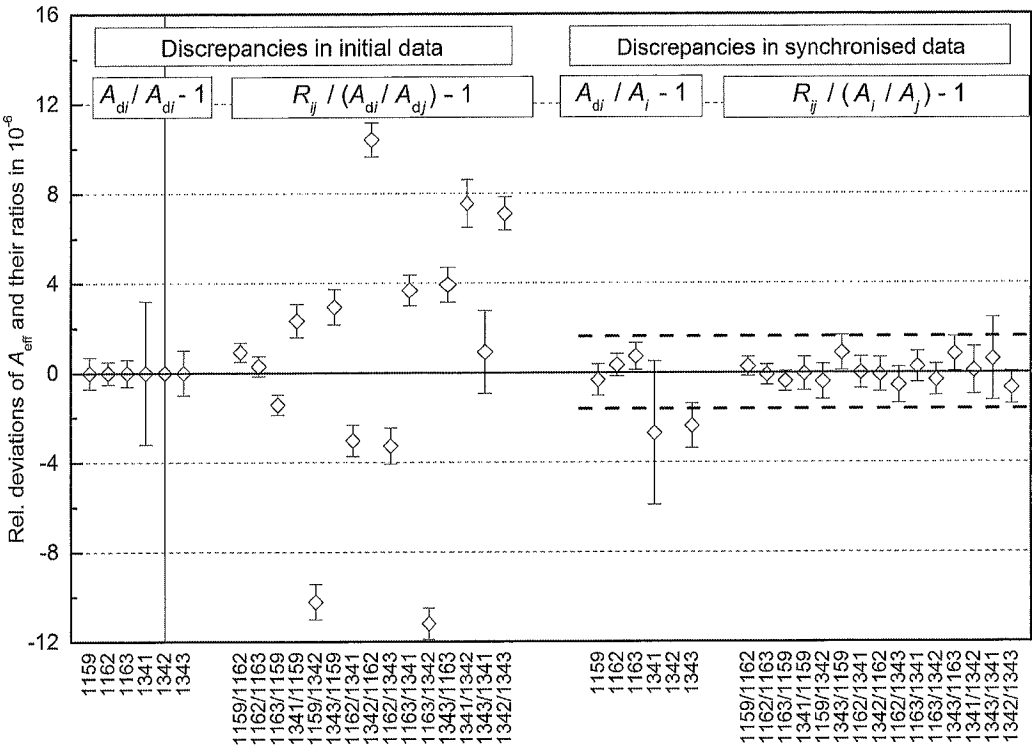

Figure 10. Left half: discrepancies between the dimensional (A_{di}, A_{di}/A_{dj}) and cross-float results (R_{ij}). Right half: discrepancies between the dimensional (A_{di}), cross-float (R_{ij}), and synchronized results (A_i). The vertical bars represent the confidence interval corresponding to the standard uncertainties of A_{di} (u_{di}) and A_i (u_i), respectively.

(ii) Comparison of the analytic solution of the synchronization (equations (4)) with the iterative calculation described in [1].
(iii) Change of the weighting in equations (2) and (3): omission of the factor 2.
(iv) Use of cross-float ratios measured at pressures up to only 1 MPa as input data for the synchronization to reduce the influence of the pressure distortion coefficients.

In all four cases, the differences between the alternative synchronization results were well within the standard uncertainty.

The values listed in table 4 show two important facts. First, the deviations between the results of the two cross-float measurements campaigns are well within the combined standard uncertainty. Since the measurements of the first campaign were performed with nitrogen as the measuring gas, this means that the effective areas are equal for helium and nitrogen at a level of order 1 ppm. Second, except for PCU No. 1343, the results of the second campaign yielded uncertainties u_i, which are significantly smaller than those of the first campaign by a factor of up to 1.7. This is especially important for PCU No. 1342, which was used in the DCGT measurements for the determination of the Boltzmann constant [16]. The reduction of the uncertainties has mainly three causes: (1) The uncertainties of several cross-float ratios are smaller, see table 1. (2) The amount of data is essentially larger, not only due to the adding of a sixth PCU. (3) The Type B components are estimated applying formulas following directly from uncertainty propagation, see the already in [14] presented smaller uncertainty estimates.

Furthermore, it is worth mentioning the following details concerning uncertainty estimates. The rough estimation of the pressure distortion coefficient of PCU 1341 causes

Table 5. Uncertainty budget for the measurement of a helium pressure of 7 MPa using PCU No. 1342 with an effective area of 2 cm^2.

	2014	2011 [9]
Component	$u(p)/p$ in ppm	$u(p)/p$ in ppm
Zero-pressure effective area	0.8_8	1.5
Pressure-distortion coefficient	0.3	1.1
Mass measurement (piston, mass pieces)	0.1	0.1
Gravity acceleration	0.1	0.1
Temperature measurement	0.2	0.2
Verticality of the PCU	0.1	0.1
Combined standard uncertainty	0.9_8	1.9

larger uncertainties of the cross-float ratios, especially those obtained from the cross-float measurements with PCUs 1342 and 1343 at higher pressures up to 7 MPa, see table 1. The estimate of $u_{\mathrm{d}i}$ for PCU 1343 is obviously too optimistic, which causes the largest $u_{\mathrm{A}i}$ estimate. On the contrary, the very large estimate for $u_{\mathrm{d}i}$ of PCU 1342, see table 3, makes the first term of the numerator in equation (5) negligible and thus $u_{\mathrm{A}1342}$ very small. This is the reason why this PCU shows the smallest uncertainty among the three 2 cm^2 PCUs. Due to the large uncertainty estimate, PCU 1342 does not really contribute to the final effective-area values of the PCUs. Its effective area comes from the other PCUs. It might be, therefore, reasonable to not include PCU 1342 in the synchronization, and to calibrate this PCU against the other five PCUs with the synchronized effective areas. But in this procedure, the synchronization complicates the consideration of correlations. Ignoring correlations, the procedure would yield an uncertainty estimate for the weighted-mean value of A_{1342} of only 0.5_5 ppm, which is smaller than the estimate given in table 4 by about one third. Thus, the inclusion of PCU 1342 in the synchronization has the advantage that well-derived formulas can be used for the uncertainty estimation, and a more reliable estimate is achieved.

5. Uncertainty budget

For the determination of the Boltzmann constant by DCGT described in [16], the PCU No. 1342 was used. Therefore, in table 5, a complete uncertainty budget for the measurement of a helium pressure of 7 MPa using PCU No. 1342 is presented. This budget is similar to that given in [9], but the first two components are now essentially smaller. The relative standard uncertainty of the zero-pressure effective area amounts now to 0.8_8 ppm (instead of 1.5 ppm), see table 4. The component caused by the uncertainty of the pressure distortion coefficient is reduced from 1.1 ppm to 0.3 ppm. This component has been estimated from the cross-float results obtained for the pair of PCUs Nos. 1342 and 1343 shown in figure 8. The A_{1342} values change by about 1 ppm from the lowest pressures to the maximum pressure of about 7 MPa. This could be caused by a mismatch of the pressure distortion coefficients calculated for the two PCUs. The application of a rectangular distribution to this change yields an estimate of about 0.3 ppm. The component caused by the temperature measurement was estimated comparing the readings of two PRTs. The resulting combined uncertainty of 0.9_8 ppm is clearly dominated by the first component.

6. Conclusions and outlook

Comprehensive cross-float experiments and the synchronization of the effective areas of a system of six special pressure balances have decreased the uncertainty of the measurement of absolute pressures up to 7 MPa compared with previous achievements presented in [1]. It is now possible to measure a helium pressure of 7 MPa with a relative standard uncertainty of 1.0 ppm applying a 2 cm^2 piston-cylinder unit, the calibration of which is traceable to the SI base units. This result is of crucial importance for dielectric-constant gas thermometry. It decreases the uncertainty of the value of the Boltzmann constant determined in 2013 [16] to 4.0 ppm, and a further reduction to below 3 ppm seems to be possible [4].

References

[1] Sabuga W 2011 *PTB-Mitt.* **121** 247–55
[2] www.bipm.org
[3] www.bipm.org/cc/CCT/Allowed/Summary_reports/recommendation_web_version.pdf
[4] Gaiser C 2015 *Metrologia* **52** S217–26
[5] Sabuga W *et al* 2011 *PTB-Mitt.* **121** 256–9
[6] Priruenrom T 2011 *Development of Pressure Balances for Absolute Pressure Measurement in Gases up to 7 MPa* (Clausthal-Zellerfeld: Papierflieger Verlag)
[7] Sabuga W *et al* 2012 *Measurement* **45** 2464–8
[8] Sabuga W *et al* 2011 *PTB-Mitt.* **121** 260–2
[9] Fellmuth B *et al* 2011 *Metrologia* **48** 1–9
[10] Johnson D P and Newhall D H 1953 *Trans. Am. Soc. Mech. Eng.* **75** 301–10
[11] Rendle C G 1993/1994 *Metrologia* **30** 611–3
[12] Sutton C M *et al* 1999 *Metrologia* **36** 517–20
[13] Kojima M *et al* 2005 *Metrologia* **42** 227–30
[14] Sabuga W and Priruenrom T 2014 *MAPAN-J. Metrol. Soc. India* (doi:10.1007/s12647-014-0116-y)
[15] Stock M *et al* 2006 *Metrologia* **43** 03001
[16] Gaiser C *et al* 2013 *Metrologia* **50** L7–11